

NEW INSIGHTS AND PRACTICAL CONSIDERATIONS IN HYPERSPECTRAL CHANGE DETECTION

M. Pieper and D. Manolakis

T. Cooley

*M. Brueggeman, A. Weisner,
and J. Jacobson*

MIT Lincoln Laboratory
244 Wood Street
Lexington, MA 02420-9185
dmanolakis@ll.mit.edu

Air Force Research Laboratory
Space Vehicles Directorate
3550 Aberdeen Ave SE
Kirtland AFB, NM 87117

National Air and Space
Intelligence Center
Wright-Patterson AFB
OH 45433

ABSTRACT

There are a multitude of civilian and military applications for the detection of anomalous changes in hyperspectral images. Anomalous changes occur when the material within a pixel is replaced. Environmental factors that change over time, such as illumination, will affect the radiance of all the pixels in a scene, despite the materials within remaining constant. The goal of an anomalous change detection algorithm is to suppress changes caused by the environment, and detect pixels where the materials within have changed.

Anomalous change detection is a two step process. Two co-registered images of a scene are first transformed to maximize the overall correlation between the images, then an anomalous change detector (ACD) is applied to the transformed images. The transforms maximize the correlation between the two images to attenuate the environmental differences that distract from the anomalous changes of importance.

Several categories of transforms with different optimization parameters are discussed and compared. One of two types of ACDs are then applied to the transformed images. The first ACD uses the difference of the two transformed images. The second concatenates the spectra of two images and uses an aggregated ACD. A comparison of the two ACD methods and their effectiveness with the different transforms is done for the first time.

Index Terms—hyperspectral, anomalous change detection

1. INTRODUCTION

Remote change detection using hyperspectral imaging data is a broad area with many civilian and military applications. In

This work is sponsored by the Air Force Research Laboratory under Air Force Contract #FA8721-05-C-0002. Opinions, interpretations, conclusions, and recommendations are those of the author and are not necessarily endorsed by the United States Government.

this paper we consider a special class of change detection applications concerned with “small” and “anomalous” changes [1, 2]; a review of techniques for general image change detection is given by [3]. In *anomalous change detection* (ACD) problems two hyperspectral images of the same scene, taken at different times and under different conditions are available. The objective is to detect small objects that have been inserted, deleted, or moved between the two observations. The data may be registered with a one-to-one correspondence between pixels of the same location [4]. Environmental changes and radiance changes due to illumination are of no interest.

The basic assumptions underlying the operation of hyperspectral change detection algorithms are: (a) the background clutter and environmental conditions in the two images are correlated; therefore, we can predict one from the other; (b) “small” and “anomalous” changes in one image constitute “new” information which cannot be predicted from the other image. Therefore, a reasonable approach to change detection shown in Fig. 1 involves two steps: (a) transform the two images to bring out their overall similarities; (b) use an ACD algorithm to find differences between the two transformed images.

The paper is organized as follows, in Section 2 several image transforms are discussed, then the ACD algorithms are discussed in Section 3. A comparison of the results using the different permutations of image transforms and ACD algorithms is given in Section 4 for an AFRL change detection test. The conclusions are discussed in Section 5.

2. IMAGE TRANSFORMS

Due to environmental changes, the pixel radiances of the two images taken of a scene at different times will differ. However, the materials within most pixels remain consistent so that there is a correlation between the images. Linear transforms are applied to each of the images to attenuate the subtle changes caused by time, and bring out the correlation between the pixel materials of the two images. For unchanged pixels,

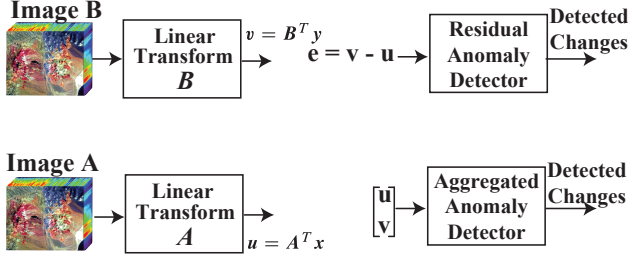


Fig. 1. Generalized framework for change detection.

the differences between the transformed spectra from the two images should be small. When the material in a pixel is replaced by an anomalous man-made material, the correlation between the pixel pair is lost, causing a large spectral change allowing for detection.

The transformed spectra are

$$v = B^T y \text{ and } u = A^T x \quad (1)$$

where x is a $p \times 1$ pixel spectrum in the first image and y is a corresponding $q \times 1$ pixel spectrum in the second image. The mean vectors $m_x = E(x)$, $m_y = E(y)$ are assumed to both be 0 and the covariance matrices of the images

$$C = \text{cov} \left(\begin{bmatrix} x \\ y \end{bmatrix} \right) = \begin{bmatrix} C_x & C_{xy} \\ C_{yx} & C_y \end{bmatrix} \quad (2)$$

are assumed known. The transforms A and B , are $p \times r$ and $q \times r$ matrices, where $r \leq \min(p, q)$. Table 1 shows the A and B transforms derived in [5] [6] [7] from optimizing different criteria.

Method	A	B	Required quantities
Linear Prediction-X	I	$C_y^{-1} C_{yx}$	C_x, C_y, C_{xy}
Linear Prediction-Y	$C_x^{-1} C_{xy}$	I	C_x, C_y, C_{xy}
CCA	$C_x^{-1/2} P$	$C_y^{-1/2} Q$	$\tilde{C}_{xy} = PDQ^T$
Modified CCA	$C_x^{-1/2} PD$	$C_y^{-1/2} Q$	$\tilde{C}_{xy} = PDQ^T$
SVD	P_0	Q_0	$C_{xy} = P_0 D_0 Q_0^T$
PCA	P_1	Q_2	$C_x = P_1 D_1 Q_1^T$ $C_y = P_2 D_2 Q_2^T$
CE	$P_1 D_1^{-1/2}$	$Q_2 D_2^{-1/2}$	$C_x = P_1 D_1 Q_1^T$ $C_y = P_2 D_2 Q_2^T$

where $\tilde{C}_{xy} \stackrel{\delta}{=} C_x^{-1/2} C_{xy} C_y^{-1/2}$ and $\text{svd}(C) = PDQ^T$

Table 1. Summary of image transforms.

The Linear Prediction-X and Y minimize the MSE in either the X or Y full spectral spaces [5]. The rest of the transforms reduce the dimensionality of the transformed images by maximizing either the correlation or variance of orthogonal components. Canonical Correlation Analysis (CCA) finds

relationships of how the two images are most correlated [6]. Modified-CCA minimizes the MSE between the two CCA spaces by bringing one canonical space into the other using the canonical correlation coefficients in the diagonal of D . The SVD transform based on C_{xy} maximizes the variance in one image explained by the other [7]. Individual PCA transforms which don't use C_{xy} are less sensitive to image mis-registration. The maximum variance components that explain the relatively consistent image materials are highly correlated, and are similar to the SVD transform components. Covariance Equalization (CE) whitens along the principal components of each image by equally weighting each component [5].

3. ANOMALOUS CHANGE DETECTION

Anomalous differences are detected by comparing the pixels of the two transformed images in one of several ways. In this section the methods used to find three ACD scores d_1 , d_2 , and d_3 are discussed. In the first method, the difference between the two transformed images is taken and an anomaly detector (AD) is run on the residual image

$$d_1 = e^T C_e^{-1} e \text{ where the residual image is } e = v - u \quad (3)$$

The second method is uses the aggregated image AD, defined in [8]

$$d_2 = \begin{bmatrix} u \\ v \end{bmatrix}^T G^{-1} \begin{bmatrix} u \\ v \end{bmatrix} \quad (4)$$

where the aggregated covariance is

$$G = \text{cov} \left(\begin{bmatrix} u \\ v \end{bmatrix} \right) = \begin{bmatrix} G_u & G_{uv} \\ G_{vu} & G_v \end{bmatrix} \quad (5)$$

and its inverse is

$$G^{-1} = \begin{bmatrix} -G_{u|v}^{-1} & G_u^{-1} G_{uv} G_{v|u}^{-1} \\ G_{v|u}^{-1} G_{vu} G_u^{-1} & G_v^{-1} \end{bmatrix} \quad (6)$$

where

$$G_{u|v} = G_u - G_{uv} G_v^{-1} G_{vu} \text{ and } G_{v|u} = G_v - G_{vu} G_u^{-1} G_{uv} \quad (7)$$

The aggregated image AD can be simplified to

$$d_2 = (u - \hat{u})^T G_{u|v}^{-1} u + (v - \hat{v})^T G_{v|u}^{-1} v \quad (8)$$

$\hat{u}^T = v^T G_v^{-1} G_{vu}$ is a linear prediction of v to u and

$\hat{v}^T = u^T G_u^{-1} G_{uv}$ is a linear prediction of u to v .

The last method considered is the Hyperbolic Anomalous Change Detector (HACD), which takes the aggregated image AD and subtracts each image AD [8]

$$d_3 = d_2 - u^T G_u^{-1} u - v^T G_v^{-1} v \quad (9)$$

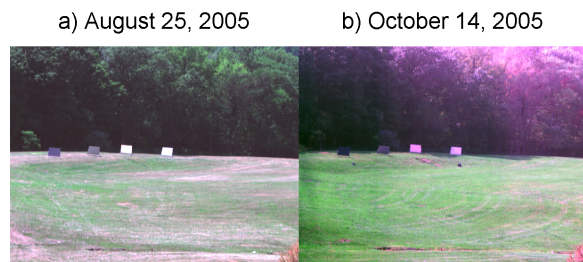


Fig. 2. Images of test scene

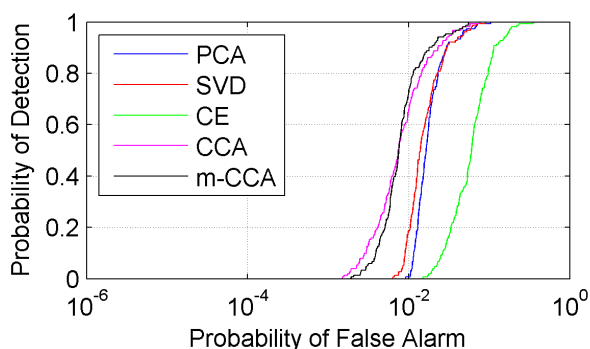


Fig. 3. ROC curves for the residual error AD.

4. RESULTS

The image transforms and anomalous change detection algorithms discussed in the previous sections were tested on two hyperspectral images collected by AFRL for a change detection test. The images shown in Fig. 2a and 2b were collected on August 25 and October 14, 2005 between which noticeable environmental changes occurred. Both images contain 4 anomalous panels in front of the trees. The October image has two black tarps inserted in the grass below the panels. The two tarps are anomalous changes of interest that must be found with as few false alarms as possible. The images were taken with a stationary hyperspectral imager allowing for optimal image registration [9].

Following the framework in Fig. 1 the August and October images were transformed using one of the last six image transforms in Table 1. The first 10 components of each of the transformed image pairs were then processed with each of the ACD algorithms. Using ground truth for the black tarp pixel locations, receiver operating characteristic (ROC) curves were created for each of the anomalous change detection and transform pair results. The ROC curves for the residual error, aggregated image, and HACD are shown in Fig. 3, 4, and 5.

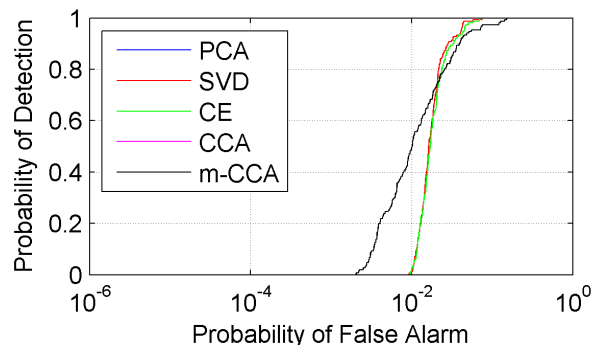


Fig. 4. ROC curves for the aggregated image AD.

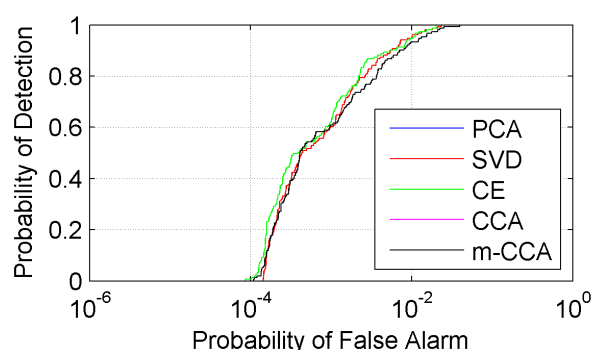


Fig. 5. ROC curves for the HACD.

The mean ACD scores of the black tarps and the third panel from the left for each combination of image transform and ACD algorithm are shown in Table 2. To compared the ACD scores of the black tarps and panel to the background scores the mean and standard deviation of the whole ACD images are also shown in Table 2.

	ACD	PCA	SVD	CE	CCA	m-CCA
Black Tarp Mean	Residual Error	47.38	44.65	26.01	49.78	55.06
	Aggregated	83.42	88.27	83.42	74.55	74.55
	Hyperbolic	53.98	56.68	53.98	54.02	54.02
Panel Mean	Residual Error	145.9	136.5	155.0	20.53	19.27
	Aggregated	264.4	286.5	264.5	95.69	95.69
	Hyperbolic	-18.73	-28.63	-18.73	-28.21	-28.21
Image Mean	Residual Error	10.00	10.00	10.00	10.00	10.00
	Aggregated	20.00	20.00	20.00	20.00	20.00
	Hyperbolic	0	0	0	0	0
Image STD	Residual Error	13.29	15.42	12.78	11.01	10.48
	Aggregated	26.72	28.25	26.71	20.53	20.53
	Hyperbolic	9.18	9.94	9.18	10.27	10.27

Table 2. Anomalous Change Detection Image Scores

In order for an ACD to be effective, the scores of the black tarps should be higher than the anomalous panels present in both of the images. For the residual error ACD, the CCA and m-CCA maximized the correlation between the two transformed images and were the only transforms that showed effective suppression of the anomalous panel compared to the black change tarps. The ACD mean score of the black tarp was twice that of the panel providing the best ROC curves in Fig. 3. The similar PCA and SVD transform components provided similar ROC curves. CE which is PCA with equal component weights was the worst because the variability of the first few components explained the scene and the black tarps and were weighted less.

The aggregated ACD was ineffective at suppressing the anomalous panels. The CCA and m-CCA showed more comparable scores for the black tarps and panel, which explained the slightly better ROC curves in Fig. 4. The transform pairs PCA/CE and CCA/m-CCA have identical orthogonal components that are either unweighted/weighted. After the whitening of the aggregated ACD, the transform pairs give identical statistics and ROC curves. The aggregated ACD gives the highest ACD scores because the aggregated image has double the spectral dimensionality of the residual image, which also doubles the ACD image mean score shown in Table 2.

The HACD is an aggregated ACD with each image AD subtracted. The image ADs have half the spectral dimensionality of the aggregated image and half the ACD image mean score. When the two image ADs are subtracted from the aggregated ACD, the mean becomes centered at 0. The shared anomalies in both of the images are subtracted twice, and are suppressed with negative values, as shown for the panel in Table 2. The black tarp mean scores are comparable to the means for the residual error, and the suppression of the shared anomalies provides the best ROC curves of all the ACD algorithms. The HACD ROC curves for the different image transforms were nearly identical.

5. CONCLUSION

Each ACD procedure had similar problems. False alarms were caused by drastic illumination changes and the anomalous panels in both of the scenes. In addition, the black change tarps were difficult to find with a single image AD. The goal was to determine which transform and AD pair was most effective at balancing the suppression of the possible false alarms while still enhancing the changes caused by the introduction of the black tarps in the scene.

The CCA transforms with the residual AD showed the greatest suppression of the anomalous panels, but the black panel statistics were not much higher resulting in a high P_{FA} . The aggregated AD enhanced the black tarp changes for all the transforms, however, the anomalous panels were barely suppressed. The HACD ROC curves for each of the transforms were nearly identical and showed the best results of

all the detection methods. The black tarps were visible with each transform and the false alarms of the aggregated AD were suppressed by subtracting the anomalies in both images. Anomalous changes detected by either single image AD were suppressed, but not by enough to make them undetectable.

References

- [1] Michael T. Eismann, Joseph Meola, Alan D. Stocker, Scott G. Beaven, and Alan P. Schaum, "Airborne hyperspectral detection of small changes," *Appl. Opt.*, vol. 47, no. 28, pp. F27–F45, 2008.
- [2] James Theiler, "Quantitative comparison of quadratic covariance-based anomalous change detectors," *Appl. Opt.*, vol. 47, no. 28, pp. F12–F26, 2008.
- [3] Richard J Radke, Srinivas Andra, Omar Al-Kofahi, and Badrinath Roysam, "Image change detection algorithms: a systematic survey," *Image Processing, IEEE Transactions on*, vol. 14, no. 3, pp. 294–307, 2005.
- [4] Barbara Zitova and Jan Flusser, "Image registration methods: a survey," *Image and vision computing*, vol. 21, no. 11, pp. 977–1000, 2003.
- [5] A Schaum and A Stocker, "Linear chromodynamics models for hyperspectral target detection," in *Aerospace Conference, Proceedings. IEEE*, 2003, vol. 4, pp. 4_1879–4_1885.
- [6] A. Rencher, *Multivariate Statistical Inference and Applications*, Wiley Series in Probability and Statistics. John Wiley & Sons, Inc., New York, 1998.
- [7] Steve Cherry, "Singular value decomposition analysis and canonical correlation analysis," *Journal of Climate*, vol. 9, no. 9, pp. 2003–2009, 1996.
- [8] J. Theiler, C. Scovel, B. Wohlberg, and B.R. Foy, "Elliptically contoured distributions for anomalous change detection in hyperspectral imagery," *Geoscience and Remote Sensing Letters, IEEE*, vol. 7, no. 2, pp. 271–275, April 2010.
- [9] Joseph Meola, Michael T. Eismann, Kenneth J. Barnard, and Russell C. Hardie, "Analysis of hyperspectral change detection as affected by vegetation and illumination variations," *Proc. SPIE*, 2007, vol. 6565.